

POLITECNICO DI TORINO
Repository ISTITUZIONALE

Assessment of unbalance and distortion components in three-phase systems with harmonics and interharmonics

Original

Assessment of unbalance and distortion components in three-phase systems with harmonics and interharmonics / Chicco, Gianfranco; Russo, Angela; Pons, Enrico; Spertino, Filippo; Porumb, Radu; Postolache, Petru; Toader, Cornel. - In: ELECTRIC POWER SYSTEMS RESEARCH. - ISSN 0378-7796. - STAMPA. - 147:(2017), pp. 201-212.
[10.1016/j.epsr.2017.02.016]

Availability:

This version is available at: 11583/2666868 since: 2020-01-29T12:35:09Z

Publisher:

Elsevier

Published

DOI:10.1016/j.epsr.2017.02.016

Terms of use:

This article is made available under terms and conditions as specified in the corresponding bibliographic description in the repository

Publisher copyright

(Article begins on next page)

Assessment of unbalance and distortion components in three-phase systems with harmonics and interharmonics

Gianfranco Chicco^a, Enrico Pons^a, Angela Russo^{a,*}, Filippo Spertino^a, Radu Porumb^b, Petru Postolache^b, Cornel Toader^b

^a Politecnico di Torino, Dipartimento Energia, corso Duca degli Abruzzi 24, 10129 Torino, Italy

^b Universitatea Politehnica din Bucuresti, Facultatea Energetica, Splaiul Independentei 313, Bucharest, Romania

ABSTRACT

This paper deals with the identification of balance, unbalance and distortion components in unbalanced three-phase systems with distorted waveforms containing harmonics and interharmonics. The analysis starts from the harmonic distortion and unbalance components found through the symmetrical component-based (SCB) approach previously defined by the authors. The SCB approach is extended in this paper by introducing an auxiliary reference frequency and identifying its consistency condition with respect to the fundamental system frequency. After defining the auxiliary reference frequency, the proposed approach directly uses the classical symmetrical component transformation matrix at any harmonic or interharmonic. Various results are presented, for conventional test cases and for measurements gathered from real systems with variable unbalanced and distorted loads. These results show that the extended SCB approach is particularly useful to analyze three-phase systems in unbalanced and distorted conditions with harmonics and interharmonics, because of its simplicity and intuitiveness compared to other approaches.

Keywords:
Unbalanced three-phase systems
Harmonics
Interharmonics
Symmetrical components

1. Introduction

A three-phase system with periodic phase current waveforms (period T) is defined as *balanced* if the phase current waveforms are equal in shape, are regularly shifted in time of $T/3$ and the sequence of phase rotation is conventional (i.e., counterclockwise). Otherwise, the three-phase system is *unbalanced*. The definition of balance works regardless of the possible waveform distortion with respect to the sinusoid at the fundamental frequency. The classical definition of unbalance, i.e., the ratio between the negative and the positive sequence components, takes into account only the components at the fundamental frequency. Likewise, the classical definition of the total harmonic distortion (THD) refers to balanced three-phase systems only. However, in practice, unbalance, harmonics and interharmonics [1] are simultaneously present in actual systems.

The extraction of information concerning the levels of unbalance and distortion in three-phase systems with neutral has been addressed recently. First and second unbalance components have been determined in [2] by considering harmonic distortion,

resorting to different transformation matrices applied at different harmonic orders; however, these two components have no individual physical meaning and are combined together to represent the system unbalance. The symmetrical component transformation has been applied in [3] to study the harmonic distortion due to fluorescent lamps, by considering only odd harmonics and providing a simple formulation of the neutral-to-phase current ratio in a particular case. Furthermore, the approach of [2] has been applied in [4] to extend the definition of apparent power based on symmetrical components to the case of non-sinusoidal waveforms.

In [5] the symmetrical component-based (SCB) approach has been introduced to exploit the same transformation matrix from phase quantities into symmetrical components to separate balance, unbalance and distortion components. The rationale for this separation is based on the fact that a balanced waveform may contain components at different harmonics, and the balance components are obtained by picking up selected entries of the transformed voltage and current vectors at different harmonic orders. The unbalance components are directly taken from the complementary entries calculated by using the same transformation matrix, without the need to create the first and second unbalance components. The SCB balance, unbalance and distortion components are defined as sums of squared RMS values of the transformed components at

* Corresponding author.

each harmonic order [6]. The SCB approach has been applied in [7] to characterize the harmonic distortion in photovoltaic systems with different types of unbalance (that is, structural unbalance, unbalance from partial shading, and mixed unbalance).

Recently, the approach used in [2] has been extended in [8] and [9] to take into account interharmonics, again using different versions of the transformation matrices. An application of this method of evaluation of unbalanced and distorted components has been presented in [10] to characterize the disturbance compensation obtained by active power filters. Furthermore, in [11] the use of the Discrete-Wavelet transform has been proposed to evaluate the symmetrical components. This approach has shown to be adequate also for studying non-stationary distorted and unbalanced waveforms. The effects of unbalance, harmonics, and interharmonics on phase-locked loop systems (PLL) have been analyzed in [12], resulting in the proposal of analytical formulas that characterize the PLL phase angle and frequency errors in the presence of disturbances.

Following the same rationale used in [8], the main contribution of this paper is to extend the SCB approach to take into account interharmonics, providing a simple identification of the balance, unbalance and distortion components. This extension is presented for the general case of distorted waveforms with harmonics and interharmonics, when the output from the measurement system is gathered by using a proper sampling rate in the frequency domain. The consistency conditions for proper sampling are established in this paper by introducing an auxiliary reference frequency in the general case. The sampling rate is then chosen in a way consistent with current standards, in particular with Standard IEC 61000-4-7 [13] defining the harmonic and interharmonic groups and sub-groups. Finally, the balance, unbalance and distortion indicators are calculated with the extended SCB approach on the basis of their corresponding components.

The rest of the paper is organized as follows. Section 2 introduces the general hypotheses used in the approach presented in this paper to deal with harmonics and interharmonics in balanced systems. Section 3 illustrates the extension of the SCB indicators to interharmonics for a general unbalanced system with distorted waveforms. Section 4 shows some examples of application to test cases and real-case measurements, highlighting the calculation of the various components and indicators. The last section contains the concluding remarks.

2. Assessment of the sequences in a balanced system

Let us first consider a balanced three-phase system, in which the waveforms gathered in the time domain are subject to the Fast Fourier Transform (FFT) in order to obtain the related components in the frequency domain.

Let us formulate the frequency axis partitioning in two different ways:

- partitioning according to the nominal system frequency $f_1 = 50 \text{ Hz}$ (or 60 Hz), associated to the variable f_h for the harmonic order $h = 1, \dots, H$, with frequency variation step Δf_h ;
- partitioning depending on the rate used for sampling the waveform in the harmonics domain, that is, 5 Hz for $f_1 = 50 \text{ Hz}$ (i.e., 10 periods for a total of 200 ms , while 12 periods are used for $f_1 = 60 \text{ Hz}$) as indicated in the Standard IEC 61000-4-7, associated to the auxiliary variable \hat{f}_z for $z = 1, \dots, N_z$, with frequency variation step $\Delta \hat{f}_z$.

Let us now assume that the following *consistency conditions* are satisfied for any integer $k = 0, 1, 2, \dots$:

$$H = 10^{-k} N_z \quad (1)$$

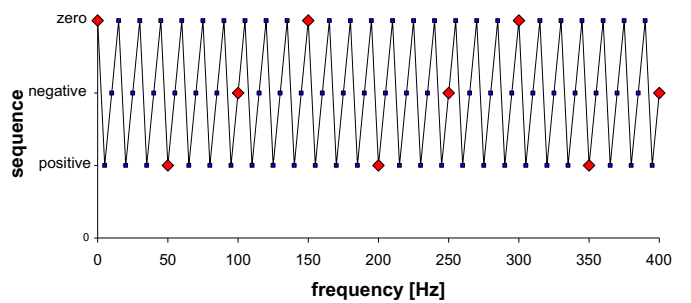


Fig. 1. Identification of the positive, negative and zero sequences for a balanced system at 5-Hz fundamental frequency (small points) and at 50-Hz fundamental frequency (large points).

$$\Delta f_h = 10^k \Delta \hat{f}_z \quad (2)$$

By using the FFT to process the waveform measured for a duration $T = 10^k/f_1$ with $k > 0$, the waveform components at frequency multiple of $1/T$ are seen as harmonics resulting from the FFT, but are interharmonics for the system operating at fundamental frequency f_1 [8]. Because of this, in the sequel the variable z will be denoted as interharmonic order. In particular, starting from this general condition, the case $k=0$ corresponds to the calculation carried out by considering only the harmonic orders defined at frequency f_1 , while the case $k=1$ is the one considered in the Standard IEC 61000-4-7.

The maximum interharmonic order N_z can be linked to the maximum harmonic order considered in the classical harmonic analysis, for which $H=40$ or $H=50$ are used, by applying (1). If $k=1$ the resulting values are $N_z=400$ or $N_z=500$, respectively.

By applying the SCB approach to the FFT results with auxiliary fundamental frequency $\hat{f}_1 = 5 \text{ Hz}$, if the three-phase system is balanced, the components associated with positive, negative and zero sequences are illustrated in Fig. 1. In the figure, the small points represent the frequencies drawn with the frequency variation step $\Delta \hat{f}_z$, and the large points represent the frequencies multiple of f_1 . From Fig. 1, if the consistency conditions are satisfied, the positive, negative and zero sequences assigned to the components at the frequency variation step Δf_h are fully consistent with the sequences assigned to the components at the frequency variation step $\Delta \hat{f}_z$.

The same concept is represented in Table 1, showing the sequences referring to the various harmonic orders and to the interharmonic bands defined in the standard IEC 61000-4-7 (zero frequency included).

3. Extension of the SCB indicators

3.1. Interharmonics-based balance, unbalance and distortion components

Let us now consider a general unbalanced three-phase system, in which the three phase currents at the interharmonic order $z=1, \dots, N_z$ are identified by the phasors $\mathbf{i}^z = [\bar{I}_a^z \bar{I}_b^z \bar{I}_c^z]^T$, where the superscript T denotes vector transposition. Applying the symmetrical component transformation matrix [14] with the operator $\alpha = e^{j\frac{2\pi}{3}}$, at each interharmonic order the triplet of phase current phasors is transformed into the new triplet $\mathbf{i}_T^z = [\bar{I}_{T1}^z \bar{I}_{T2}^z \bar{I}_{T3}^z]^T$, as follows:

$$\begin{vmatrix} \bar{I}_{T1}^z \\ \bar{I}_{T2}^z \\ \bar{I}_{T3}^z \end{vmatrix} = \frac{1}{3} \begin{vmatrix} 1 & \alpha & \alpha^2 \\ 1 & \alpha^2 & \alpha \\ 1 & 1 & 1 \end{vmatrix} \begin{vmatrix} \bar{I}_a^z \\ \bar{I}_b^z \\ \bar{I}_c^z \end{vmatrix} \quad (3)$$

The interharmonics-based components are defined here as in [5], by using the superscripts b for balance, u for unbalance, and d for distortion. The notion of positive, negative and zero sequences

Table 1

Identification of the sequences for the various harmonic orders and interharmonic bands according with the standard IEC 61000-4-7 (the symbols used are + for the positive sequence, – for the negative sequence, and 0 for the zero sequence).

Harmonic order	0	1	2	3	4	5	6	7	8	9	10	11	12	13	14	15	16	17	18	19	20
Interharmonic band	0	1	–	0	+	–	0	+	–	0	+	–	0	+	–	0	+	–	0	+	–
Sequence (interharmonic)	0	+	–	0	+	–	0	+	–	0	+	–	0	+	–	0	+	–	0	+	–
Sequence (harmonic)	0																				
Harmonic order																					
Interharmonic band	21	22	23	24	25	26	27	28	29	30	31	32	33	34	35	36	37	38	39	40	4
Sequence (interharmonic)	0	+	–	0	+	–	0	+	–	0	+	–	0	+	–	0	+	–	0	+	+
Sequence (harmonic)	0									0											

for the balanced system is exploited to define the balance phase current component, with superscripts referring to the interharmonic order z :

$$\hat{I}_p^b = \sqrt{\sum_{z=1}^{N_z} \left[(I_{T1}^{3z-2})^2 + (I_{T2}^{3z-1})^2 + (I_{T3}^{3z-3})^2 \right]} \quad (4)$$

For $z = 1, \dots, N_z$, the balance phase current component depends only on three terms. In fact, if the system is *balanced*:

- only the phasors of the harmonic orders 1, 4, 7, … (i.e., $3z - 2$), representing the positive sequence components captured by I_{T1}^{3z-2} , may be non-null;
- only the phasors of the harmonic orders 2, 5, 8, … (i.e., $3z - 1$), representing the negative sequence components captured by I_{T2}^{3z-1} , may be non-null;
- only the phasors of the harmonic orders 3, 6, 9, … (i.e., $3z - 3$), representing the zero sequence components captured by I_{T3}^{3z-3} , may be non-null.

The unbalance phase current component is defined by considering all the other terms:

$$\hat{I}_p^u = \sqrt{\sum_{z=1}^{N_z} \left[(I_{T2}^{3z-2})^2 + (I_{T3}^{3z-2})^2 + (I_{T1}^{3z-1})^2 + (I_{T3}^{3z-1})^2 + (I_{T1}^{3z-3})^2 + (I_{T2}^{3z-3})^2 \right]} \quad (5)$$

Finally, the phase current distortion component collects all the components at interharmonic orders others than the fundamental harmonic (corresponding to $z = 10^k$, from Section 2):

$$\hat{I}_p^d = \sqrt{\sum_{\substack{z=0 \\ z \neq 10^k}}^{N_z} \left[(I_{T1}^z)^2 + (I_{T2}^z)^2 + (I_{T3}^z)^2 \right]} \quad (6)$$

The same concepts are applied to define the components and indicators referring to the phase voltages, and to the neutral current, extending the formulation used in [5] from harmonics to interharmonics.

The balance, unbalance and distortion components introduced above are used to define the extended versions of the related indicators, that remain formally similar to those introduced in [5], the difference being in the definition of the components. For instance, the interharmonics-based balance components at fundamental frequency f_1 and referring to distortion are respectively defined as

$$\hat{I}_p^{b1} = I_{T1}^{10^k} \quad (7)$$

$$\hat{I}_p^{bd} = \sqrt{(\hat{I}_p^b)^2 - (\hat{I}_p^{b1})^2} \quad (8)$$

Furthermore, the interharmonics-based unbalance components at fundamental frequency f_1 and referring to distortion are respectively defined as

$$\hat{I}_p^{u1} = \sqrt{(I_{T2}^{10^k})^2 + (I_{T3}^{10^k})^2} \quad (9)$$

$$\hat{I}_p^{ud} = \sqrt{(\hat{I}_p^u)^2 - (\hat{I}_p^{u1})^2} \quad (10)$$

3.2. Interharmonics-based balance, unbalance and distortion indicators

The interharmonics-based indicators are defined on the basis of the components introduced above. For instance, the phase current unbalance factor referring to the balanced current at fundamental frequency is defined as

$$\hat{\psi}_{pl}^u = \frac{\hat{I}_p^u}{\hat{I}_p^{b1}} \quad (11)$$

while the representation of the *classical unbalance factor*, in which the components are calculated at the fundamental frequency f_1 , is

$$\hat{\psi}_{pl}^{u1} = \frac{\hat{I}_p^{u1}}{\hat{I}_p^{b1}} \quad (12)$$

In addition, the phase current balance distortion factor is defined to represent the *classical THD* for a system with no unbalance:

$$\hat{\psi}_{pl}^{bd} = \frac{\hat{I}_p^{bd}}{\hat{I}_p^{b1}} \quad (13)$$

and the phase current unbalance distortion factor is formulated as

$$\hat{\psi}_{pl}^{ud} = \frac{\hat{I}_p^{ud}}{\hat{I}_p^{b1}} \quad (14)$$

On these bases, the interharmonics-based Total Phase current Distortion ($\hat{T}PD_I$) extends the classical *THD* concept to unbalanced systems:

$$\hat{T}PD_I = \frac{\hat{I}_p^d}{\sqrt{(\hat{I}_p^{b1})^2 + (\hat{I}_p^u)^2}}, \quad (15)$$

and the interharmonics-based Total Phase current Unbalance ($\hat{T}PU_I$) indicator extends the unbalance indicator to distorted currents:

$$\hat{T}PU_I = \frac{\hat{I}_p^u}{\hat{I}_p^b} \quad (16)$$

The major differences with respect to other formulations are:

- The transformation matrix used in (3) is constant (i.e., independent of the interharmonics order) for the whole approach, enabling a direct definition of the balance, unbalance and distortion components by using the same matrix, while the

transformation matrices change in [2] at each harmonic order and in [8] at each harmonic/interharmonic order.

- (b) The unbalanced components are defined with a unique term, without defining separate first and second unbalanced components as in [2] and [8].

3.3. Interharmonics-based components and indicators for the neutral current

Following the rationale introduced in [5] and considering the symmetrical component transformation in (3), the RMS value of the neutral current is determined by collecting all the components found in the return path, that is:

$$I_n = 3 \sqrt{\sum_{z=1}^{N_z} (I_{T3}^z)^2} \quad (17)$$

The neutral current components due to phase balance, unbalance and distortion are defined in the interharmonic domain as follows, respectively:

$$\hat{I}_n^b = 3 \sqrt{\sum_{z=1}^{N_z} (I_{T3}^{3z-3})^2} \quad (18)$$

$$\hat{I}_n^u = 3 \sqrt{\sum_{z=1}^{N_z} [(I_{T3}^{3z-1})^2 + (I_{T3}^{3z-2})^2]} \quad (19)$$

$$\hat{I}_n^d = \sqrt{\sum_{\substack{z=0 \\ z \neq 10^k}}^{N_z} (I_{T3}^z)^2} \quad (20)$$

In the same way, the neutral current balance, unbalance and distortion factors are respectively defined as:

$$\hat{\psi}_{nl}^b = \frac{\hat{I}_n^b}{I_n} \quad (21)$$

$$\hat{\psi}_{nl}^u = \frac{\hat{I}_n^u}{I_n} \quad (22)$$

$$\hat{\psi}_{nl}^d = \frac{\hat{I}_n^d}{I_n} \quad (23)$$

Finally, the neutral-to-phase current ratio is defined with reference to the balance component of the phase current:

$$N\hat{T}P_l = \frac{I_n}{\hat{I}_p^b} \quad (24)$$

and the fundamental neutral-to-phase current ratio is formulated as:

$$N\hat{T}P_l^1 = \frac{I_n}{\hat{I}_p^{b1}} \quad (25)$$

4. Examples of application

4.1. Rationale of the examples presented

The first test has been carried out to confirm that the results obtained by the proposed approach in cases with harmonics only (i.e., without interharmonics) are the same obtained in the basic SCB approach. For this purpose, the illustrative examples presented in Section III of [5] have been reworked. The results match the ones reported in Table II of [5] and are not repeated here.

Then, the cases with interharmonics have been addressed. The results obtained with three types of data are presented in the sequel:

- the first set of data is defined with analytical expressions, taken from the ones used in the case studies analyzed in [8]; these expressions are rescaled in such a way that the sinusoidal components at different frequencies have a unity RMS value instead of an amplitude equal to unity as used in [8];
- the second set of data comes from measurements gathered on a real-life application in a low-voltage distribution system supplying tertiary sector loads;
- the third set of data refers to experimental results gathered during the operation of a welding system with currents circulating in two phases.

All the calculations are carried out by considering the fundamental frequency at $k=1$ and $z=10$. For the latter dataset, an example is also provided with $k=2$, in which the fundamental frequency is located at $z=100$.

4.2. Example with case studies in the presence of interharmonics of [8]

4.2.1. Description of the data

The case studies indicated in [8] are constructed by considering three interharmonic signals at 10 Hz ($z=2$, with RMS value equal to 1 per unit) added to perfectly balanced fundamental components ($z=10$, with RMS value equal to 1 per unit). Three cases are formulated, by choosing different phase angles of interharmonics:

1. *Balanced interharmonic case study*: the phase angles of interharmonics satisfy the symmetry property at 50 Hz, as introduced in [9], that is, the symmetry of the waveforms at 10 Hz and 50 Hz occurs at the same time instants in the first period of the waveforms at 50 Hz, that is, at the time instants 0, $T/3$ and $2T/3$ (Fig. 2). The expressions of the phase and neutral currents are, respectively (Fig. 3):

$$\begin{cases} i_a(t) = \sqrt{2} \cos(10\omega t) + \sqrt{2} \cos(2\omega t) \\ i_b(t) = \sqrt{2} \cos\left(10\omega t - \frac{120\pi}{180}\right) + \sqrt{2} \cos\left(2\omega t - \frac{24\pi}{180}\right) \\ i_c(t) = \sqrt{2} \cos\left(10\omega t - \frac{240\pi}{180}\right) + \sqrt{2} \cos\left(2\omega t - \frac{48\pi}{180}\right) \end{cases} \quad (26)$$

$$i_n(t) = i_a(t) + i_b(t) + i_c(t) \quad (27)$$

leading to the input phase current vectors, for $z=10$ and $z=2$, respectively:

$$\mathbf{i}^{10} = j [1 \ \alpha^2 \ \alpha]^T \quad (28)$$

$$\mathbf{i}^2 = [j \ e^{j66\pi/180} \ e^{j42\pi/180}]^T \quad (29)$$

The angles considered in (29) are complementary with respect to the angles subtracted to the component for $z=2$ in (30).

- *Unbalanced interharmonic case study*: the phase angles of interharmonics satisfy the symmetry property at 10 Hz. The neutral current is null. The expressions of the phase currents (Fig. 4) in the time domain are:

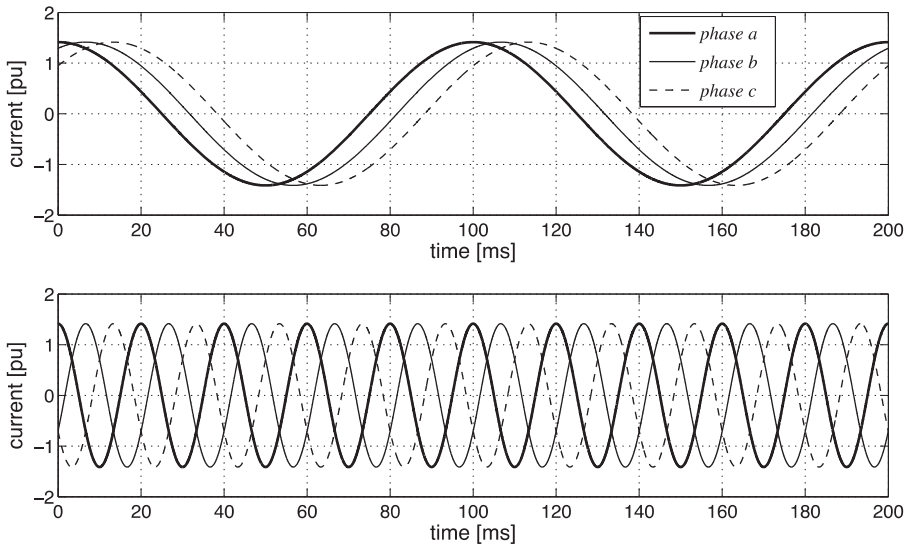


Fig. 2. Phase currents for the components at 10 Hz ($z=2$, upper graph) and at 50 Hz ($z=10$, lower graph) for the balanced interharmonic case study.

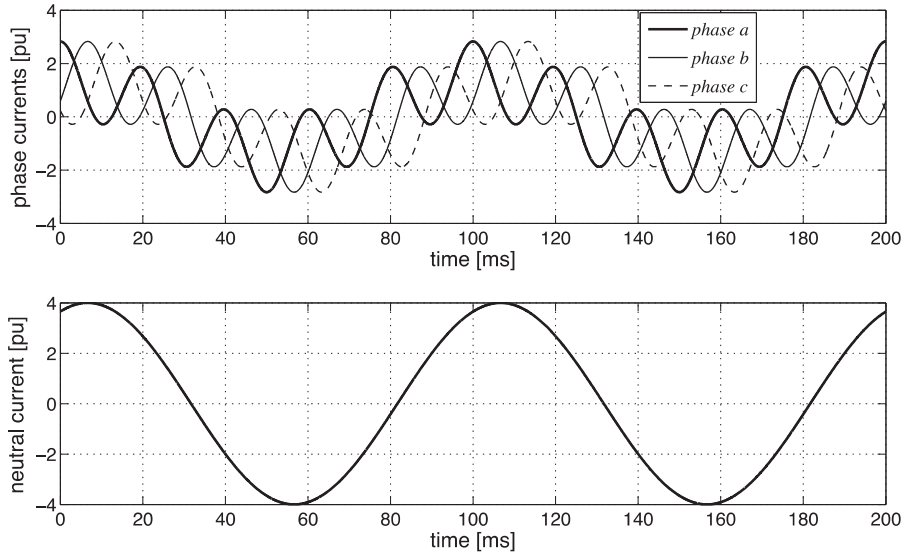


Fig. 3. Phase currents (upper graph) and neutral current (lower graph) for the balanced interharmonic case study.

$$\begin{cases} i_a(t) = \sqrt{2} \cos(10\omega t) + \sqrt{2} \cos(2\omega t) \\ i_b(t) = \sqrt{2} \cos\left(10\omega t - \frac{120\pi}{180}\right) + \sqrt{2} \cos\left(2\omega t - \frac{120\pi}{180}\right) \\ i_c(t) = \sqrt{2} \cos\left(10\omega t - \frac{240\pi}{180}\right) + \sqrt{2} \cos\left(2\omega t - \frac{240\pi}{180}\right) \end{cases} \quad (30)$$

leading to the input phase current vectors expressed as in (28) for $z=10$ and, for $z=2$:

$$\mathbf{i}^2 = j \begin{bmatrix} 1 & 1 & 1 \end{bmatrix}^T \quad (31)$$

$$\begin{cases} i_a(t) = \sqrt{2} \cos(10\omega t) + \sqrt{2} \cos(2\omega t) \\ i_b(t) = \sqrt{2} \cos\left(10\omega t - \frac{120\pi}{180}\right) + \sqrt{2} \cos(2\omega t) \\ i_c(t) = \sqrt{2} \cos\left(10\omega t - \frac{240\pi}{180}\right) + \sqrt{2} \cos(2\omega t) \end{cases} \quad (32)$$

while the neutral current follows the general expression (27) leading to the input phase current vector expressed as in (28) for $z=10$ and, for $z=2$:

$$\mathbf{i}^2 = j \begin{bmatrix} 1 & 1 & 1 \end{bmatrix}^T \quad (33)$$

4.2.2. Results of the extended SCB components and indicators in the three cases

In all the cases, for $z=10$ the phase currents at the fundamental frequency are balanced, and the transformed currents are:

$$\mathbf{i}_T^{10} = [j \ 0 \ 0]^T \quad (34)$$

- **Zero-sequence interharmonic case study:** the phase angles of interharmonics satisfy the zero-sequence symmetry property at 10 Hz. The expressions of the phase and neutral currents are (Fig. 5):

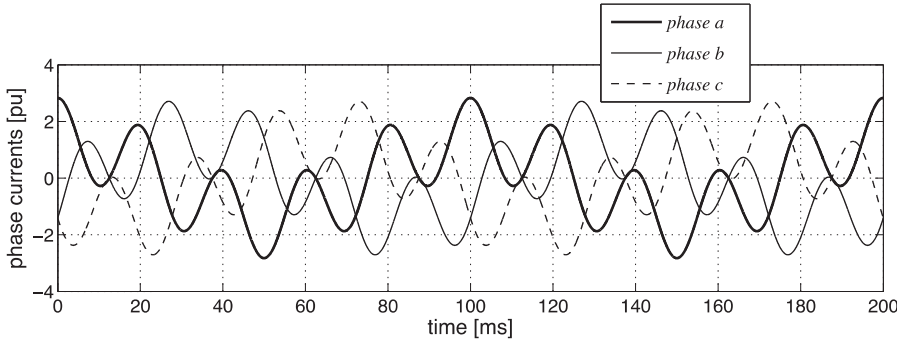


Fig. 4. Phase currents for the unbalanced interharmonic case study.

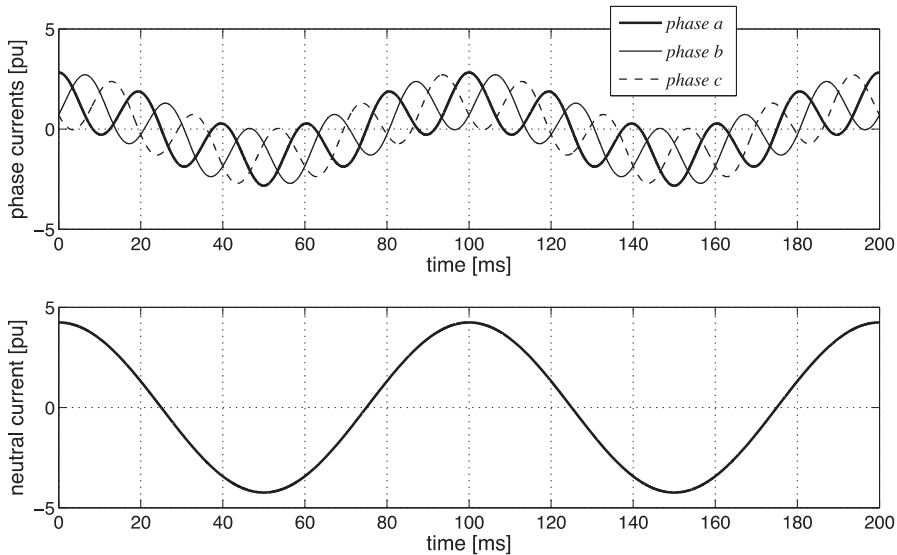


Fig. 5. Phase currents (upper graph) and neutral current (lower graph) for the zero-sequence interharmonic case study.

After the application of the symmetrical component transformation, the transformed current components at 10 Hz ($z=2$) are different for the three cases, namely:

- in the *balanced interharmonic* case:

$$\mathbf{i}_T^2 = [(0.524 + j0.736) \quad (-0.053 - j0.264) \quad (0.236 + j0.236)]^T \quad (35)$$

- in the *unbalanced interharmonic* case:

$$\mathbf{i}_T^2 = [j \quad 0 \quad 0]^T \quad (36)$$

- in the *zero-sequence interharmonic* case:

$$\mathbf{i}_T^2 = [0 \quad 0 \quad j]^T \quad (37)$$

The components and the indicators obtained by the application of the extended SCB approach are reported in [Tables 2 and 3](#), respectively. Looking at the entries reported in these tables it is possible to easily identify the characteristics of the datasets used.

In the *balanced interharmonic* case, since the distortion appears only at 10 Hz and the RMS values at 10 Hz and 50 Hz are equal, the phase current distortion \hat{I}_p^d coincides with the RMS value of the component at 10 Hz. Moreover, the phase current at 10 Hz is decomposed into non-null terms in all the entries of the vector \mathbf{i}_T^2 . Thus, both the balance distortion \hat{I}_p^{bd} and the unbalance distortion component \hat{I}_p^{ud} appear, the latter being also equal to the unbalance

component \hat{I}_p^u , as the phase currents at 50 Hz are balanced. The neutral current depends on the component at 10 Hz and is totally due to unbalance and distortion.

In the *unbalanced interharmonic* case, the transformed currents for $z=2$ and $z=10$ contain a non-null term only in the first component of the vector \mathbf{i}_T^2 . These terms correspond to a balance component for $z=10$ and to an unbalance component for $z=2$ (since a balance component would be introduced only by a non-null second entry of the vector \mathbf{i}_T^2). Furthermore, this unbalance component is also the only distortion component appearing in the waveform. The neutral current is null.

In the *zero-sequence interharmonic* case, the transformed currents for $z=2$ correspond to a non-null term only in the third component of the vector \mathbf{i}_T^2 . Again, this term introduces an unbalance component for $z=2$, which is also the only distortion component. In the same way, the neutral current is totally unbalanced and distorted.

4.3. Example with real measurements on a LV switchboard

Tertiary sector loads cover a significant share of consumption, and contain a relevant portion of non-linear loads. The measurements have been performed in the LV switchboard of a MV/LV substation feeding a portion of the University building. In particular, the monitored three-phase line feeds a canteen and a coffee shop for students and staff, in which both single-phase and three-phase appliances are used. The three line currents, the three phase

Table 2
Balance, unbalance, and distortion components in cases with interharmonics.

Component [per unit]		Case		
		Balanced interharmonic	Unbalanced interharmonic	Zero-sequence interharmonic
Balance phase current component	\hat{I}_p^b	1.021	1	1
Balance fundamental phase current component	\hat{I}_p^{b1}	1	1	1
Balance phase current distortion component	\hat{I}_p^{bd}	0.206	–	–
Unbalance phase current component	\hat{I}_p^u	0.979	1	1
Unbalance fundamental phase current component	\hat{I}_p^{u1}	–	–	–
Unbalance phase current distortion component	\hat{I}_p^{ud}	0.979	1	1
Phase current distortion	\hat{I}_p^d	1	1	1
Neutral current	I_n	2.827	–	3
Balance neutral current component	\hat{I}_n^b	–	–	–
Unbalance neutral current component	\hat{I}_n^u	2.827	–	3
Neutral current distortion component	\hat{I}_n^d	2.827	–	3

Table 3
Unbalance and harmonic distortion indicators in cases with interharmonics.

Indicator		Case		
		Balanced interharmonic	Unbalanced interharmonic	Zero-sequence interharmonic
Phase current balance distortion factor	$\hat{\psi}_{pl}^{bd}$	0.206	0	0
Phase current unbalance distortion factor	$\hat{\psi}_{pl}^{ud}$	0.979	1	1
Phase current unbalance factor at fund. frequency	$\hat{\psi}_{pl}^{u1}$	0	0	0
Phase current overall unbalance factor	$\hat{\psi}_{pl}^u$	0.979	1	1
Total phase current distortion	$T\hat{P}D_I$	1	1	1
Total phase current unbalance	$T\hat{P}U_I$	0.958	1	1
Neutral current balance factor	$\hat{\psi}_{nl}^b$	0	–	0
Neutral current unbalance factor	$\hat{\psi}_{nl}^u$	1	–	1
Neutral current distortion factor	$\hat{\psi}_{nl}^d$	1	–	1
Neutral-to-phase current ratio	$N\hat{T}P_I$	2.769	0	3
Fundamental neutral-to-phase current ratio	$N\hat{T}P_I^1$	2.827	0	3

Table 4
Current probes accuracy (example on a LV switchboard).

Range	Amplitude accuracy
1–10 A	±2%
10–100 A	±1%

voltages and the voltage between neutral and ground have been gathered by installing a network analyzer (Dranetz Powerguide 4400) immediately downstream of the circuit breaker. For voltage measurement a direct connection is possible, as the four channels are differential inputs insulated up to 600 V RMS. For what concerns the currents, three AC clamp-on probes Dranetz TR2550A have been used, which work in the range from 1 A to 100 A RMS. The accuracy characteristics of the current probes are reported in [Table 4](#).

The network analyzer is characterized by the following specifications:

- Accuracy on currents: 0.1% of the reading + accuracy of the current probes (from [Table 4](#))
- Sampling rate: 12.8 kSa/s
- Resolution: 16 bits

The measurements have been performed by recording 10 cycles of the current and voltage waveforms; the data have been stored on the memory card of the network analyzer and then downloaded and converted into the comma-separated values (CSV) format for the subsequent elaboration.

In the sequel, some results are presented with reference to three datasets corresponding to three measurements gathered at 15 min from each other, in order to capture the variable behavior of the

loads. The three datasets are indicated as *Data1*, *Data2* and *Data3*, respectively. The maximum harmonic order considered is $H=40$, corresponding to $N_Z=400$ and to the frequency 2 kHz.

[Fig. 6](#) shows the phase and neutral currents from *Data1*. This dataset is prevailingly unbalanced, with relatively low waveform distortion. [Fig. 7](#) shows the spectral components (amplitude) of the phase and neutral currents, containing a visible presence of interharmonics, especially at phase c. The high unbalance results in transferring the phase c interharmonics to a large extent to the neutral current. The system unbalance is clearly indicated by the components and indicators reported in [Tables 5 and 6](#). The phase and neutral current unbalance factors emerge as the most significant indicators, while the distortion factors are low.

[Fig. 8](#). The phase and neutral current unbalance factors emerge as the most significant indicators, while the distortion factors are low.

[Fig. 8](#) shows the phase and neutral currents from *Data2*. The corresponding waveforms are much more unbalanced than the ones of *Data1*, and the waveform distortion is again relatively low. Even though from [Table 5](#) the unbalance phase current distortion component (in ampere) has a value similar to the one of the same component in *Data1*, the RMS currents of *Data2* are lower, so the resulting $T\hat{P}U_I$ in [Table 6](#) is much higher for *Data2*. The neutral-to-phase current ratios are significantly high, with the RMS neutral current exceeding the balance phase current components.

[Fig. 9](#) shows the phase and neutral currents from *Data3*. With this dataset, from [Table 5](#) the balance phase current component is similar to the one of *Data2*, while the unbalance phase current component is much lower than in the previous datasets. The waveform distortion, indicated by the $T\hat{P}U_I$ in [Table 6](#), is similar to the other datasets for the phase current distortion, but is much higher than

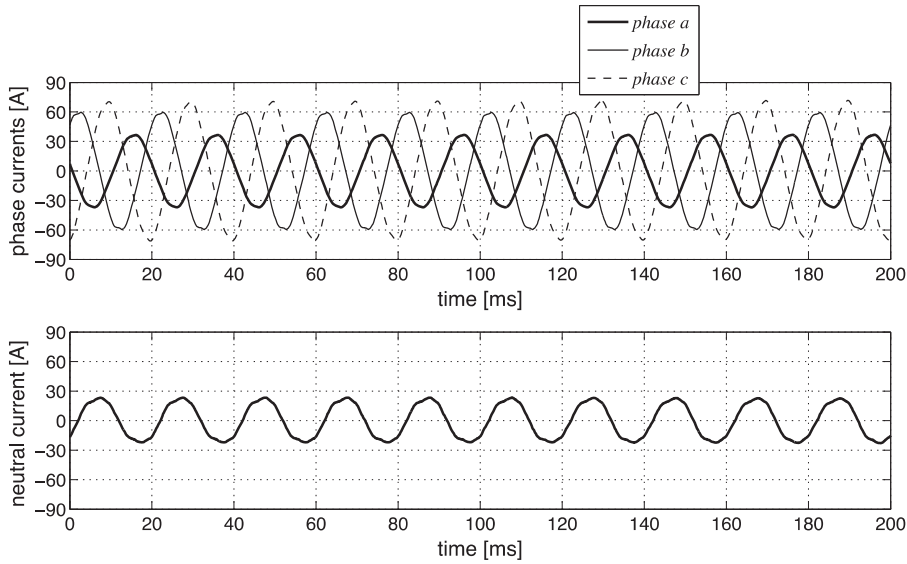


Fig. 6. Phase currents (upper graph) and neutral current (lower graph) from dataset *Data1*.

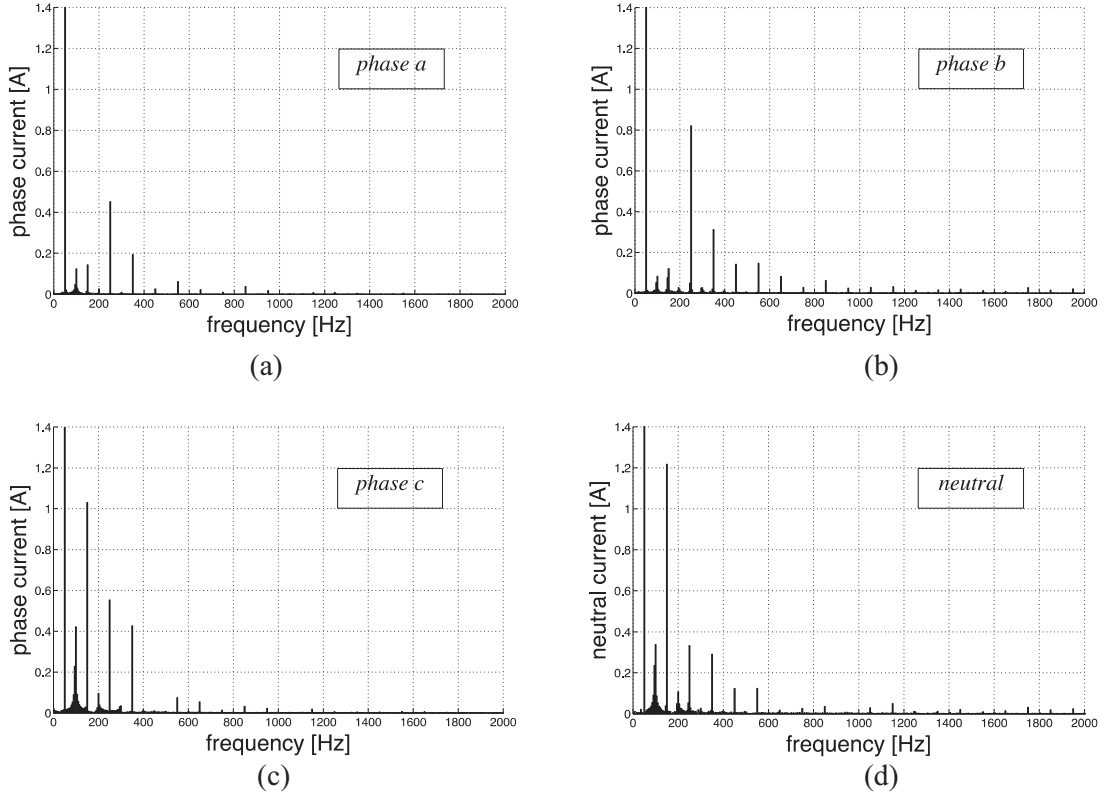


Fig. 7. Amplitude of the spectral components of phase currents (a), (b), and (c), and of the neutral current (d) for dataset *Data1*. The 50 Hz components (truncated in the figure) are 26.10 A, 42.55 A, 49.06 A, and 16.53 A, respectively.

for the other datasets for the neutral current, also with the prevailing contribution of the triplen harmonics determining the neutral current balance factor [15].

Finally, Table 7 shows the traditional harmonic distortion indicators assessed by considering the harmonic bands defined in the Standard IEC 61000-4-7 [13]. From Table 7, let us consider the dataset *Data1*. The THD of the phase currents assessed by considering only the harmonic bands are 2.05%, 2.17% and 2.70%, respectively. If also interharmonics are included in the assessment, by associating them with the nearest harmonic band, the corre-

sponding group total harmonic distortion *THDG* values reach 2.07%, 2.19% and 2.77%, respectively. From the extended SCB approach, the $\hat{T}PD$ shown in Table 6, characterizing the three-phase system and incorporating the effect of unbalance together with harmonic distortion, is 2.48%. A direct comparison among the $\hat{T}PD$ and the individual *THD* or *THDG* cannot be carried out, as the amplitudes of the phase currents are different, while the $\hat{T}PD$ is a synthetic indicator referring to the three-phase system, accounting for all the effects of harmonic distortion and unbalance. For the neutral current, the $\hat{T}PD$ is not defined, and the relevant indicator is the

Table 5

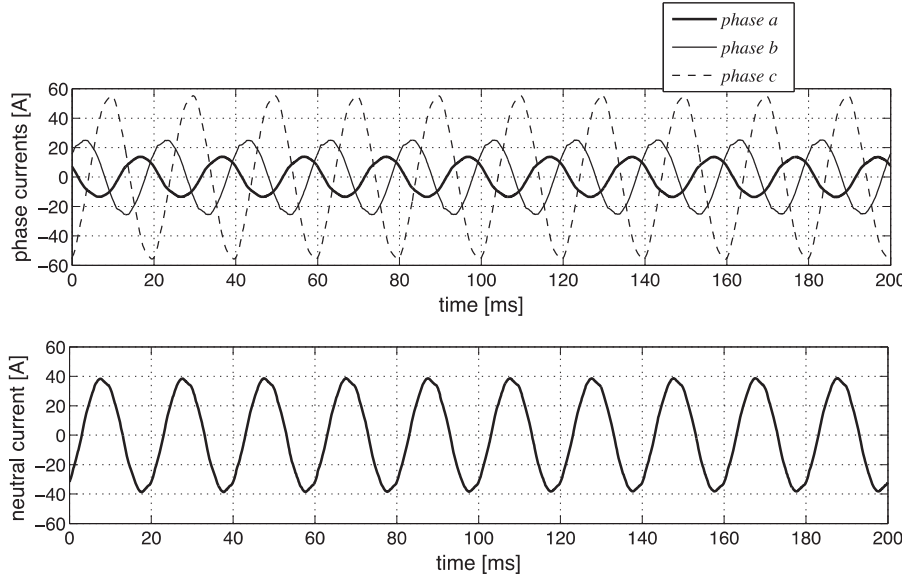
Balance, unbalance, and distortion components for real measurements on a LV switchboard.

Component	Dataset	Data1	Data2	Data3
Balance phase current component [A]	\hat{i}_p^b	39.19	22.06	21.93
Balance fundamental phase current component [A]	\hat{i}_p^{b1}	39.19	22.06	21.92
Balance phase current distortion component [A]	\hat{i}_p^{bd}	0.820	0.399	0.526
Unbalance phase current component [A]	\hat{i}_p^u	9.886	12.39	2.284
Unbalance fundamental phase current component [A]	\hat{i}_p^{u1}	9.869	12.38	2.254
Unbalance phase current distortion component [A]	\hat{i}_p^{ud}	0.574	0.525	0.366
Phase current distortion [A]	\hat{i}_p^d	1.001	0.660	0.641
Neutral current [A]	i_n	16.59	27.31	4.569
Balance neutral current component [A]	\hat{i}_n^b	1.235	0.571	0.996
Unbalance neutral current component [A]	\hat{i}_n^u	16.54	27.31	4.459
Neutral current distortion component [A]	\hat{i}_n^d	1.395	0.759	1.215

Table 6

Unbalance and harmonic distortion indicators for real measurements on a LV switchboard.

Indicator	Dataset	Data1	Data2	Data3
Phase current balance distortion factor	$\hat{\psi}_{pl}^{bd}$	0.0209	0.0181	0.0240
Phase current unbalance distortion factor	$\hat{\psi}_{pl}^{ud}$	0.0147	0.0238	0.0167
Phase current unbalance factor at fundamental frequency	$\hat{\psi}_{pl}^{u1}$	0.2519	0.5610	0.1028
Phase current overall unbalance factor	$\hat{\psi}_{pl}^u$	0.2523	0.5615	0.1042
Total phase current distortion	$T\hat{P}D_I$	0.0248	0.0261	0.0291
Total phase current unbalance	$T\hat{P}U_I$	0.2522	0.5614	0.1042
Neutral current balance factor	$\hat{\psi}_{nl}^b$	0.0744	0.0209	0.2181
Neutral current unbalance factor	$\hat{\psi}_{nl}^u$	0.9972	0.9998	0.9759
Neutral current distortion factor	$\hat{\psi}_{nl}^d$	0.0841	0.0278	0.2659
Neutral-to-phase current ratio	$N\hat{T}P_I$	0.4232	1.2379	0.2084
Fundamental neutral-to-phase current ratio	$N\hat{T}P_I^1$	0.4233	1.2381	0.2084

**Fig. 8.** Phase currents (upper graph) and neutral current (lower graph) for dataset Data2.**Table 7**Total Harmonic Distortion and Group Total Harmonic Distortion indicators for real measurements on a LV switchboard according to IEC 61000-4-7 [13], total phase current distortion $T\hat{P}D_I$, and neutral current distortion factor $\hat{\psi}_{nl}^d$.

Dataset	Data1				Data2				Data3			
Current	$i_a(t)$	$i_b(t)$	$i_c(t)$	$i_n(t)$	$i_a(t)$	$i_b(t)$	$i_c(t)$	$i_n(t)$	$i_a(t)$	$i_b(t)$	$i_c(t)$	$i_n(t)$
Total harmonic distortion (%)	2.05	2.17	2.70	8.21	4.98	3.09	2.17	2.74	2.08	2.72	3.39	26.76
Group total harmonic distortion (%)	2.07	2.19	2.77	8.44	5.02	3.19	2.21	2.78	2.17	2.86	3.57	27.55
$T\hat{P}D_I$ from Table 6 (%)	2.48	—	—	2.61	—	—	—	2.91	—	—	—	—
$\hat{\psi}_{nl}^d$ from Table 6 (%)	—	—	—	8.41	—	—	—	2.78	—	—	—	26.59

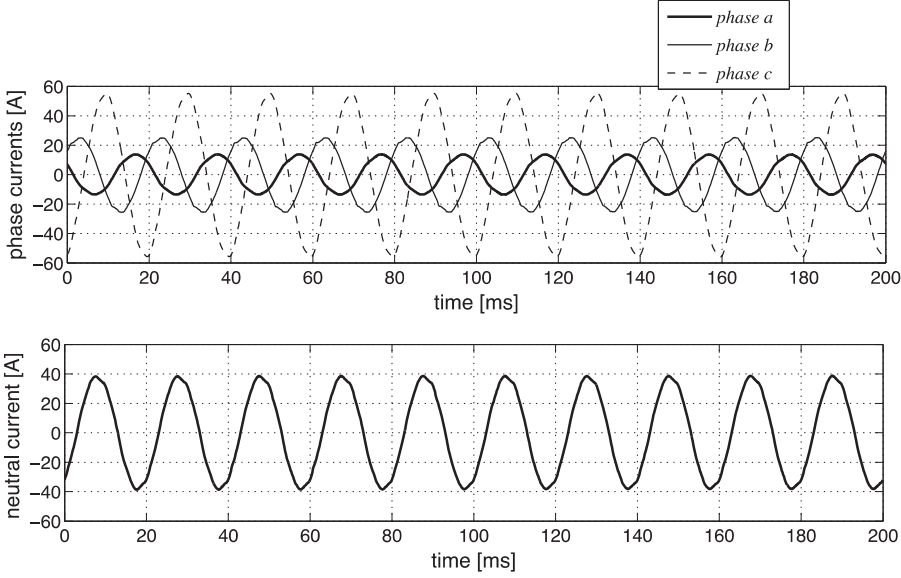


Fig. 8. Phase currents (upper graph) and neutral current (lower graph) for dataset *Data2*.

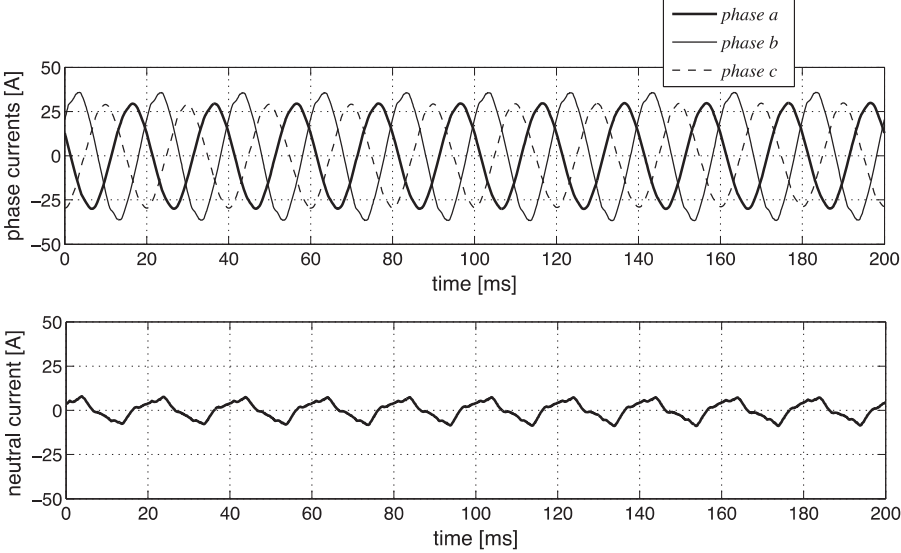


Fig. 9. Phase currents (upper graph) and neutral current (lower graph) for dataset *Data3*.

neutral current distortion factor $\hat{\psi}_{nl}^d$. Similar considerations hold for the other two datasets.

4.4. Example with real measurements on a welding system

A further example is presented here, with measurements carried out on a welding system. The welding occurs on a single-phase, but the welding machine is connected to the three-phase system through a transformer, whose primary windings are connected in the phase-to-phase mode. Thereby, the input currents from *phase a* and *phase b* are equal in amplitude but are in phase opposition, while the current from *phase c* is null. This originates heavy unbalance in the three-phase supply. The measurements have been carried out during a welding operation, with the duration of 2 s (100 cycles), and have been recorded through the automatic data acquisition system [16] characterized by the following specifications:

- Accuracy on currents: 0.1% of the reading + accuracy of the current probes $\pm 1\%$ of reading $\pm 2\text{ mA}$

- Sampling rate: 25.6 kSa/s
- Resolution: 16 bits

Fig. 10 shows the phase currents in the two phases involved in the welding process. The non-regular shape of the waveforms originates a non-negligible interharmonic content. The duration of 2 s has been chosen in order to satisfy the consistency conditions indicated in Eqs. (1) and (2) with $k=2$, corresponding to the frequency variation step $\Delta\hat{f}_z = 0.5\text{ Hz}$. Furthermore, the total duration of 2 s has been partitioned into 10 successive datasets with duration of 200 ms (10 cycles) each. **Fig. 11** shows the phase current waveforms for the first 10 cycles. The analysis carried out with $k=1$ has been repeated for each one of the 10 datasets, with the aim of highlighting the possible variations of the relevant indicators calculated.

Fig. 12 shows the amplitude of the spectral components of the current at *phase a*, obtained with frequency variation step 0.5 Hz. The frequency axis is limited to 600 Hz, as the amplitudes at higher frequencies become almost negligible. The internal zoom from 0 to

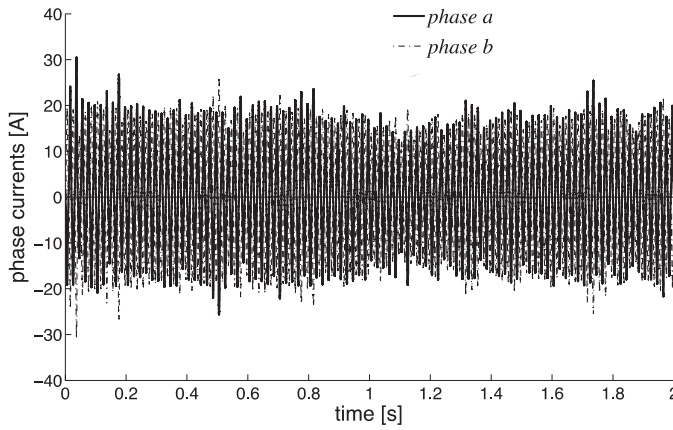


Fig. 10. Phase current waveforms for the welding case (100 cycles).

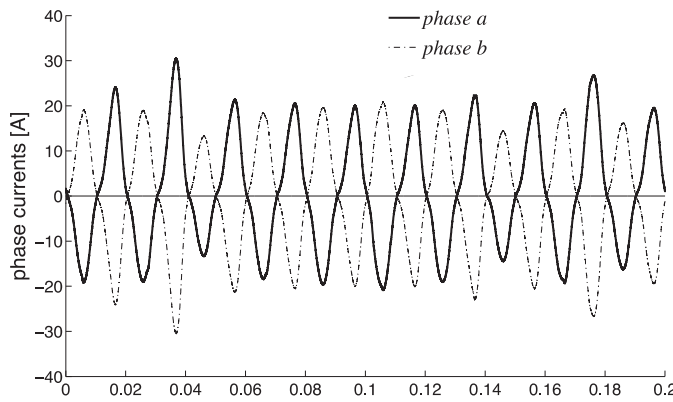


Fig. 11. Phase currents for the welding case (first 10 cycles).

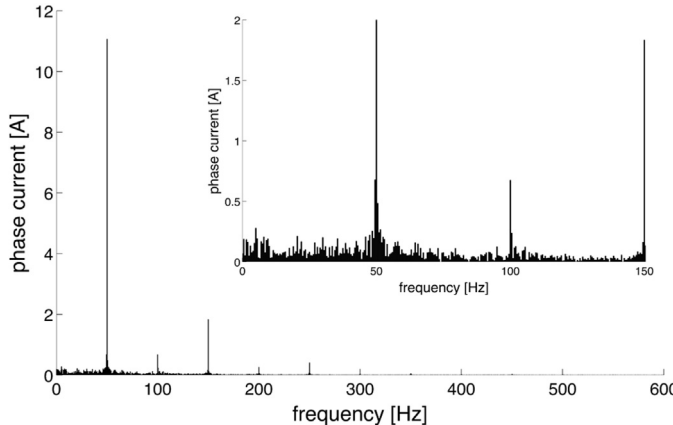


Fig. 12. Amplitude of the spectral components of the current at phase *a* for the welding case (100 cycles, frequency variation step 0.5 Hz), with internal zoom from 0 to 150 Hz (with amplitude of the component at 50 Hz truncated). The same amplitudes appear at phase *b*.

150 Hz indicates more details on the interharmonic components. The same amplitudes appear at phase *b*, because of the structural connections of the welding system. Fig. 13 contains the same information with reference to the first time interval of 10 cycles, with frequency variation step 5 Hz. The usage of the smaller frequency variation step provides greater detail in the frequency content.

The composition of the balance, unbalance and distortion indicators is carried out on the basis of the interharmonic order. Table 8 reports the balance, unbalance, and distortion components, and

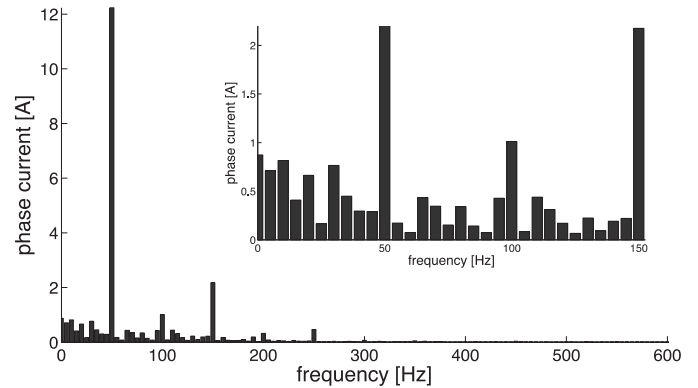


Fig. 13. Amplitude of the spectral components of the current at phase *a* for the welding case (first 10 cycles, frequency variation step 5 Hz), with internal zoom from 0 to 150 Hz (with amplitude of the component at 50 Hz truncated). The same amplitudes appear at phase *b*.

Table 8

Balance, unbalance, and distortion components for the real measurements during the welding machine operation (2 s of operation, processed with $k=2$).

Balance phase current component [A]	\hat{I}_p^b	6.45
Balance fundamental phase current component [A]	\hat{I}_p^{b1}	6.39
Balance phase current distortion component [A]	\hat{I}_p^{bd}	0.90
Unbalance phase current component [A]	\hat{I}_p^u	6.68
Unbalance fundamental phase current component [A]	\hat{I}_p^{u1}	6.39
Unbalance phase current distortion component [A]	\hat{I}_p^{ud}	1.96
Phase current distortion [A]	\hat{I}_p^d	2.16

Table 9

Unbalance and harmonic distortion indicators for real measurements during the welding machine operation (2 s of operation, processed with $k=2$).

Phase current balance distortion factor	$\hat{\psi}_{pl}^{bd}$	0.141
Phase current unbalance distortion factor	$\hat{\psi}_{pl}^{ud}$	0.307
Phase current unbalance factor at fundamental frequency	$\hat{\psi}_{pl}^{u1}$	1.000
Phase current overall unbalance factor	$\hat{\psi}_{pl}^u$	1.046
Total phase current distortion	$T\bar{P}D_I$	0.239
Total phase current unbalance	$T\bar{P}U_I$	1.036

Table 10

Total Harmonic Distortion and Group Total Harmonic Distortion indicators for real measurements during the welding machine operation (2 s of operation, processed with $k=2$), according to IEC 61000-4-7 [13], and total phase current distortion $T\bar{P}D_I$.

Current	$i_a(t)$	$i_b(t)$	$i_c(t)$
Total harmonic distortion (%)	17.8	17.8	-
Group total harmonic distortion (%)	18.8	18.8	-
$T\bar{P}D_I$ from Table 9 (%)	23.9		

Table 9 contains the corresponding indicators. From these values, it appears that the unbalance is much higher than the distortion. In the situation in which the fundamental frequency components of the two phase currents are equal (in amplitude) with opposite sign and the third phase current is null, the conventional unbalance indicator $\hat{\psi}_{pl}^{u1}$ is equal to unity. By adding the dependence on the waveform distortion, the indicator $T\bar{P}U_I$ increases to 1.036. Table 10 shows the comparison between the values of THD and $THDG$ of the phase currents, calculated according to the Standard IEC 61000-4-7 without considering unbalance, and the indicator $T\bar{P}D_I$. In this case, the $T\bar{P}D_I$ reaches higher values than THD and $THDG$, by taking unbalance into account in this particular case in which phase *c* has null current and undetermined harmonic distortion.

Fig. 14 shows the indicators obtained from the analysis of the overall 2-seconds period (frequency variation step 0.5 Hz, $k=2$) and from the 10 successive time intervals of 10 cycles each (fre-

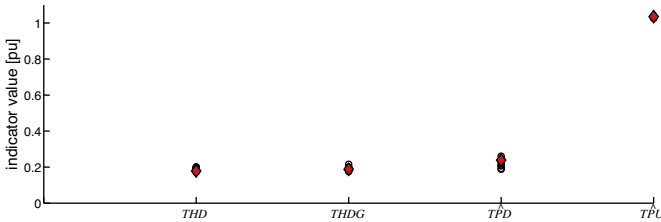


Fig. 14. Comparisons among the indicators obtained from the analysis of the 2-s period (frequency resolution 0.5 Hz, $k=2$, filled marker) and from the 10 successive time intervals of 10 cycles each (frequency resolution 5 Hz, $k=1$, empty circle markers).

quency variation step 5 Hz, $k=1$) taken from the same 2-s measured data. The time intervals of 10 cycles provide non-identical results, because the welding process is non-stationary. The indicators defined from the 2-s period fall inside the corresponding 10 points obtained from the individual 10 cycles, as the evaluations over a longer time period result in smoothing the possible higher variations occurring in the shorter individual time segments.

5. Conclusions

This paper introduced the extension of the balance, unbalance and distortion components and indicators identified in the SCB approach to waveforms containing harmonics and interharmonics. This extension, based on the definition of an auxiliary reference frequency, is consistent with previous results concerning harmonics, provided that the specific consistency condition is satisfied. The conventional components may be calculated by using measured values, gathered according to the existing power quality standards such as IEC Standard 61000-4-7. The proposed calculation of the harmonic and interharmonic entries makes it possible to take into account all the values measured at the different frequency bands to calculate the various components and indicators. In general, if the frequency of a waveform component is a non-integer multiple of the fundamental frequency, but is an integer multiple of the frequency resolution, the component can be detected by spectral analysis; otherwise (if it is a non-integer multiple of the frequency resolution), its effect will be spread between the adjacent interharmonic frequency bands.

The indicators are simple to construct by using the classical symmetrical component transformation matrix, and are easy to interpret due to the straightforward construction of the balance, unbalance and distortion terms. The examples of application presented confirmed the effectiveness of the proposed formulation.

The analysis reported in this paper considered the system currents. Similar developments can be carried out for voltages. On this basis, it is possible to define the equivalent voltages and currents for the three-phase system, as well as conventional balance and unbalance components of the apparent power. Specific terms can also be identified referring to waveform distortion, according to the indications shown in [2] and [8] for the formulations based on the

first and second unbalance, and in [5] for the components based on the SCB approach.

Acknowledgments

The authors gratefully acknowledge the technical support of Mr. Franco Quarona of Politecnico di Torino, Dipartimento Energia, during the experimental tests.

References

- [1] IEEE Task Force on Harmonics Modeling and Simulation, "Interharmonics: theory and modeling", *IEEE Trans. Power Deliv.* 22 (October) (2007) 2335–2348.
- [2] T. Zheng, E.B. Makram, A.A. Girgis, Evaluating power system unbalance in the presence of harmonic distortion", *IEEE Trans. Power Deliv.* 18 (April (2)) (2003) 393–397.
- [3] J.J.M. Desmet, I. Sweertvaegher, G. Vanalme, K. Stockman, R.J.M. Belmans, Analysis of the neutral conductor current in a three-phase supplied network with nonlinear single-phase loads, *IEEE Trans. Ind. Appl.* 39 (May/June (3)) (2003) 587–593.
- [4] O. Boudebouz, A. Boukadoum, S. Leulmi, Effective apparent power definition based on sequence components for non-sinusoidal electric power quantities, *Electr. Power Syst. Res.* 117 (December) (2014) 210–218.
- [5] G. Chicco, P. Postolache, C. Toader, Analysis of three-phase systems with neutral under distorted and unbalanced conditions in the symmetrical component-based framework, *IEEE Trans. Power Deliv.* 22 (January (1)) (2007) 674–683.
- [6] G. Chicco, R. Porumb, P. Postolache, C. Toader, Characterization of unbalanced and distorted distribution systems from experimental data, in: Proc. 15th IEEE Mediterranean Electrotechnical Conference (Melecon 2010), Valletta, Malta, April 26–28, 2010, pp. 154–159.
- [7] G. Chicco, F. Corona, R. Porumb, F. Spertino, Experimental indicators of current unbalance in building integrated photovoltaic systems, *IEEE J. Photovolt.* 4 (May (3)) (2014) 924–934.
- [8] R. Langella, A. Testa, A.E. Emanuel, Unbalance analysis for electrical power systems in the presence of harmonics and interharmonics, *IEEE International Workshop on Applied Measurements for Power Systems (AMPS)* (2011).
- [9] R. Langella, A. Testa, A.E. Emanuel, Unbalance definition for electrical power systems in the presence of harmonics and interharmonics, *IEEE Trans. Instrum. Meas.* 61 (October (10)) (2012) 2622–2631.
- [10] J. Prieto Thomas, P. Salmerón Revuelta, A. Pérez Vallés, S. Pérez Litrán, Practical evaluation of unbalance and harmonic distortion in power conditioning, *Electr. Power Syst. Res.* 141 (December) (2016) 487–499.
- [11] W.G. Morsi, M.E. El-Hawary, On the application of wavelet transform for symmetrical components computations in the presence of stationary and non-stationary power quality disturbances, *Electr. Power Syst. Res.* 81 (July (7)) (2011) 1373–1380.
- [12] L. Feola, R. Langella, A. Testa, On the effects of unbalances, harmonics and interharmonics on PLL systems, *IEEE Trans. Instrum. Meas.* 62 (September (9)) (2013) 2399–2409.
- [13] International Electrotechnical Commission, Electromagnetic Compatibility (EMC) – Part 4-7: Testing and Measurement Techniques – General Guide on Harmonics and Interharmonics Measurements and Instrumentation, for Power Supply Systems and Equipment Connected Thereto, 2009, IEC 61000-4-7, Ed. 2.1.
- [14] C.L. Fortescue, Method of symmetrical coordinates applied to the solution of polyphase networks, *Trans. AIEE pt. II* 37 (June) (1918) 1027–1140.
- [15] G. Chicco, P. Postolache, C. Toader, Triplen harmonics: myths and reality, *Electr. Power Syst. Res.* 81 (July (7)) (2011) 1541–1549.
- [16] F. Spertino, J. Ahmad, A. Ciocia, P. Di Leo, A.F. Murtaza, M. Chiaberge, Capacitor charging method for $I-V$ curve tracer and MPPT in photovoltaic systems, *Solar Energy* 119 (September) (2015) 461–473.